scientific reports

Check for updates

OPEN

Exploring the antitrypanosomal potential of rosemary root endophytic fungi with metabolomic profiling and molecular docking insights

Adel M. Abd El-kader[1,2,10], Enas Reda Abdelaleem[3,10], Yaser A. Mostafa[4], Nizar H. Saeedi[5], Ruqaiah I. Bedaiwi[5], Ramadan Yahia[6,7], Stefanie P. Glaeser[8], Peter Kämpfer[8], Omnia Magdy Hendawy[9], Usama Ramadan Abdelmohsen[1,3]✉ & Alshymaa Abdel-Rahman Gomaa[3]

Nature has been considered an interesting source of secondary bioactive compounds. Plants and their associated endophytes are common sources for these active constituents. Our study demonstrates the metabolomics profiling of the ethyl acetate extracts of three endophytic fungi associated with rosemary roots (*Cladosporium* spp., *Alternaria* spp. and *Talaromyces* spp.) in addition to the in vitro evaluation of the antitrypanosomal potential. The results revealed the presence of 47 metabolites from different chemical classes such as terpenes, phenolics, alkaloids, polyketides, macrolides, and others. Furthermore, the extracts of *Cladosporium*, *Alternaria* and *Talaromyces* exhibited potential inhibitory effects against *T. brucei* with IC_{50} values of 1.3, 3.2 and 3.5 µg/mL, respectively. Supporting the study, the identified compounds were docked against two proteins: Rhodesain in complex with a macrolactam inhibitor and ornithine decarboxylase in complex with a c-terminal fragment of antizyme. The docking simulations showed that most of the identified compounds have moderate to comparable docking score (S = − 3.82 to − 6.10 kcal/mol) within rhodesain active site. In addition, they showed weak to moderate docking scores (− 2.33 to − 5.9 kcal/mol) with a differential docking profile within ornithine decarboxylase active site. According to these findings, fungal endophytes associated with rosemary roots can be considered as a promising source of antitrypanosomal bioactive metabolites.

Keywords Rosemary, *Cladosporium*, *Alternaria*, *Talaromyces*, Metabolomics, Antitrypanosomal, Molecular docking

Natural products have been utilized as medicines for several years. Microorganisms, in addition to plants, are considered a significant source of natural compounds with desirable bioactive effects. One of the most significant categories of eukaryotic organisms being investigated for metabolites with potential for use in medicine is fungi. Grisseofulvin, cyclosporine A, taxol, β-lactam antibiotics, lovastatin and ergot alkaloids are examples of existing medications with a fungal origin[1].

[1]Department of Pharmacognosy, Faculty of Pharmacy, Deraya University, Minia 61111, Egypt. [2]Department of Pharmacognosy, Faculty of Pharmacy, Al-Azhar University, Assiut 71524, Egypt. [3]Department of Pharmacognosy, Faculty of Pharmacy, Minia University, Minia 61519, Egypt. [4]Department of Pharmaceutical Organic Chemistry, Faculty of Pharmacy, Assiut University, Assiut 71526, Egypt. [5]Department of Medical Laboratory Technology, Faculty of Applied Medical Sciences, University of Tabuk, Tabuk, Saudi Arabia. [6]Department of Microbiology and Immunology, Faculty of Pharmacy, Deraya University, Universities Zone, New Minya City 61111, Egypt. [7]Department of Microbiology and Immunology, Faculty of Pharmacy, Badr University in Assiut, 77771 Assiut, Egypt. [8]Institute of Applied Microbiology, Justus-Liebig University Gießen, Gießen, Germany. [9]Department of Pharmacology, Faculty of Pharmacy, Jouf University, Sakakah, Jouf, Saudi Arabia. [10]Adel M. Abd El-kader and Enas Reda Abdelaleem contributed equally to this work. ✉email: usama.ramadan@mu.edu.eg

Plant endophytes have gained more attention from taxonomists, ecologists, mycologists, chemists and evolutionary biologists over the last three decades. Fungal endophytes are microbes that live in the internal tissues of living plants without immediately showing any detrimental consequences, but they may become dangerous when the host plant ages[2]. The endophyte's relationship with its host plant is still unclear, but it occasionally can be identified as a mutualistic one in which the plant serves as a provider of nutrition and protection for the microorganisms, which can then produce bioactive substances that help the plant grow and survive in a variety of environments that may be harsh to the plant[3]. Most endophytes are transmitted horizontally by airborne spores to their host plants. However, some endophytes may also be vertically passed on to the subsequent plant generations by seeds. According to recent advancements in screening technologies, endophytic fungal metabolites exhibit a diversity of biological properties such as anticancer, antibacterial, antifungal, antitrypanosomal and antiviral activities and these activities are attributed to the unique products of plant endophytic fungi including terpenoids, steroids , alkaloids, and cyclopeptides that have a promising potential uses in medicine[2,4,5].

The exploration of bioactive chemicals derived from natural sources has been prompted by the rise in infections (bacteria and fungi) that are resistant to the available antimicrobials and the loss of efficacy to antiprotozoal treatment. In this regard, secondary metabolites discovered from endophytic fungi may contribute to the prevention of parasite and microbe resistance[5].

African Trypanosomiasis or sleeping sickness is an important infectious disease which affects wild and domestic animals as well as humans and it is considered one of the fetal neglected tropical diseases and threatens more than 65 million people in sub-Saharan Africa[6]. The causative agent of the disease is the parasitic protozoan, *T. brucei* which is transmitted by the bite of infected tsetse flies (*Glossina* sp.). There are two subspecies of the parasite, which are morphologically identical, and have different severity degrees of trypanosomiasis on humans. In eastern and southern Africa, the *T. brucei rhodesiense* strain causes a more severe form of acute African trypanosomiasis, while in western and central Africa, the *T. brucei gambiense* strain causes a condition that worsens over time[7]. Accordingly, there is an urgent need for the discovery of novel, safe, effective, and affordable medications with new mechanisms of action because the currently available medications have a history of ineffectiveness, resistance, and toxicity. Reviewing literatures, the plant derived secondary metabolites including terpenes, alkaloids, flavonoids, and steroids exhibited antitrypanosomal activities[8]. In addition, recent studies reported a great biosynthetic capacity of endophytic fungi to provide a prospective therapeutic candidate to combat these lethal parasites including *Alternaria sp*, *Penicillium sp*, *Exserohilum rostratum*, and *Aspergillus fumigatus*[5,9–11].

Consequently, we decided to focus our investigation of antitrypanosomal activity of three fungal strains associated with rosemary roots (Lamiaceae). Furthermore, screening the chemical profile of the fungal extracts using LC-HR-ESI-MS-based metabolomics followed by in silico molecular docking.

Material and methods

Plant material

Healthy fresh *Rosmarinus officinalis* roots (20 g) were collected in November 2023 from El-Orman botanical garden, Cairo, Egypt (30° 01′ 45′′ N 31° 12′ 47′′ E) and were verified by Prof. Dr. Nasser Barakat (Professor of Botany, Faculty of Science, Minia University). A voucher specimen (Mn-ph-Cog-075) was deposited at the Herbarium of Pharmacognosy Department, Faculty of Pharmacy, Minia University, Minia, Egypt.

Isolation and purification of endophytic fungi strains

Following a previously described protocol of isolation[12,13], the endophytic fungal strains were isolated from the inner roots tissues under sterile conditions with some modifications. In which the fresh collected plant roots were washed with tap water for 5 min then washed with sterilized distilled water for another 5 min, the roots then were soaked in ethanol 70% for 2 min and then finally washed with distilled sterilized water. After that, the roots were dissected with a sterile scalpel under aseptic conditions and surface placed on Potato Dextrose Agar (PDA, 200-g potato extract, 20 g glucose, and 15 g agar–agar powder in 1 L distilled water, PH 6.0) supplemented with Gentamycin (100 mg/L) and amoxicillin (100 mg/L) to suppress any bacterial growth and incubated at 30 °C for up to two weeks and monitored frequently for any growth. Each pure fungal colony was isolated, and surface streaked again till obtaining pure fungal isolates with distinct morphological characteristics. A glycerol stock was kept at − 70 °C for each purified strain.

Molecular identification and phylogenetic analysis

Genetic identification of the fungal strains was performed by sequence analysis of the partial 18S rRNA gene and the internal transcribed spacer (ITS) region including ITS1, the 5.8S rRNA gene, and ITS2 sequences according to Sayed et al.[14] and Mohie el-dien et al.[15]. In brief, DNA was extracted from fungal biomass using the MasterPure Yeast DNA extraction kit (epientre, Madison, Wisconsin). DNA amplification of both, the 18S rRNA gene and ITS region, was performed with universal fungal primers NS1[16] and ITS-4[17]. Sanger sequencing was performed with NS1 for the partial 18S rRNA gene sequences and with primer ITS-4 for the ITS sequences. Sequencing was performed by LGC Genomics (Berlin, Germany). Manual sequence corrections and phylogenetic analysis were performed with MEGA11 version 11.0.1[18,19]. Next related taxa were determined by BLASTN analysis against the 18S rRNA gene and ITS RefSeq Targeted Loci project databases (BioProjects PRJNA39195 and PRJNA177353; updated both at the 2023/11/06) provided in the BLASTn tool of the NCBI (https://www.ncbi.nlm.nih.gov/). ITS sequences of next related reference strains were imported into MEGA11 and aligned with ClustalW[20]. All nucleotide positions were considered with uniform rates; sequences were compared with pairwise deletions. The phylogenetic trees were constructed with the maximum likelihood method and the General Time Reversible model (for the 18S rRNA gene[21]) or the Kimura 2-parameter model (for the ITS sequence[22]). The phylogenies

were tested by the bootstrap method (100 replications). A total of 63 sequences and 1079 nucleotide positions were considered for the 18S rRNA gene sequence analysis and 64 sequences with 593 nucleotide positions for the ITS sequences. All sequences obtained from the isolated fungal strains were deposited in GenBank/EMBL/DDBJ with Accession numbers OR778281 to OR778283 (18S rRNA gene sequences) and OR785416 to OR785418 (ITS sequences).

Fungal strains fermentation and extract preparation

Fermentation (large scale) were carried out on solid rice medium (prepared by adding 100 mL of distilled water to 100 g rice in a 1 L Erlenmeyer flask and macerated overnight before autoclaving) as follows: each pure identified fungal strain in this study were cultured on PDA agar and incubated until healthy growth was obtained then, a ratio of 1.5 plate of each strain were added to every 1 sterilized rice flask and kept at room temperature for 30 days. After that, the fermentation of the fungus on the rice was stopped by adding ethyl acetate in a quantity sufficient to immerse the fermented rice. After that, the rice was crushed into small pieces as possible, and the extraction proceeded three times in three days till complete exhaustion. The ethyl acetate extract was then filtered out and evaporated by a rotary evaporator[23].

Metabolomic analysis

The ethyl acetate extract of each fungal strain was dissolved in methanol (1 mg/mL) for mass spectrometry analysis. Then they were subjected to metabolomic analysis using LC-HR-ESI–MS in accordance with previously described method[23]. The LC-HR-MS analysis was performed using an Acquity Ultra Performance Liquid Chromatography system and a Synapt G2 HDMS quadrupole time-of-flight hybrid mass spectrometer (Waters, Milford, MA, USA). BEH C18 column was adjusted to 40 °C then connected to the guard column to be ready to inject the sample (2 µL). A spray voltage of 4.5 kV was used together with both positive and negative ionization modes. Set the mass range to *m/z* 150–1500 and the capillary temperature to 320 °C. The MS dataset was processed, and data were extracted using open source software, MZmine 2.20[24] based on the established parameter. The processed data set was next subjected to molecular formula prediction and peak identification. The corresponding extract's positive and negative ionization mode data sets were dereplicated against DNP (Dictionary of Natural products) and MarinLit.

In silico study

In-silico molecular docking simulations were performed within crystal structure of two proteins; Rhodesain in complex with a macrolactam inhibitor, (3~{S})-19-chloranyl-~{N}-(1-cyanocyclopropyl)-8-methoxy-5-oxidanylidene-12,17-dioxa-4-azatricyclo[16.2.2.0^{6,11}]do-cosa-1(20),6(11),7,9,18,21-hexaene-3-carboxamide (PDB ID: 6EXQ)[25], and ornithine decarboxylase in complex with a c-terminal fragment of antizyme (PDB ID: 4ZGY); using Molecular Operating Environment (MOE) software (2012), (access date: Sept. 30, 2023)[26]. Preparation of ligands, proteins, and docking protocols were done as previously published[27]. Validation of prepared protein was achieved by re-docking of co-crystallized ligand, and it revealed acceptable docking score at RMSD values of 0.69 and 1.03 A for 6EXQ and 4ZGY: respectively.

In vitro antitrypanosomal activity

According to Huber and Koella's protocol, the antitrypanosomal activity was evaluated[28]. In brief, *T. brucei brucei* strain TC 221 was introduced to complete Baltz medium at a concentration of 10^4 trypanosomes per ml. Trypanosomes were evaluated in 96-well plate chambers using test extracts at varying concentrations of 10–200 µg/mL in 1% DMSO to a final volume of 200 µL. Afterwards, the parasites and 1% DMSO were added simultaneously to each plate as a control, along with no test extracts, to demonstrate that the 1% DMSO had no effect. In a CO_2 incubator (CelMateVR, ESCOTM, Singapore), the plates were inoculated with the test extracts and then incubated for 24 h at 37 °C in a 5% CO_2 atmosphere. Then, 20 µL of Alamar Blue was added, and after 48 and 72 h, the activity was assessed by measuring the light absorption with an MR 700 Microplate Reader at a wavelength of 550 nm and a reference wavelength of 650 nm. The test extracts' IC_{50} values were calculated using linear interpolation of three separate measurements. Suramin (IC_{50} 0.23 µg/mL) was utilized as a positive control.

Results and discussion

Phylogenetic diversity of fungi associated with rosemary roots

Based on the phylogenetic analysis of partial 18S rRNA gene sequences and the ITS sequences, the three studied fungi were placed to three different genera. Strain UR1 was identified as *Cladosporium* sp. with highest 18S rRNA gene (99.6%) and ITS (100%) sequence similarity to *Cladosporium sphaerospermum* CBS 193.54 (type material). Strain UR2 was placed into the genus *Alternaria* with high sequence similarities to different species of the genus if 18S rRNA gene sequences were compared (>99%); highest ITS sequence similarity was obtained to *Alternaria papavericola* CBS 116,606 with 99%. ITS sequence similarities to all other *Alternaria* spp. was below 99%. The third strain represented a *Talaromyces* sp. with high partial 18S rRNA gene sequence similarities to several *Talaromyces* spp. (>99%). At the ITS level highest sequence similarity was obtained to *Talaromyces stititatus* (98.34%), while sequence similarities to all other *Talaromyces* spp. were below 98%. The phylogenetic placement of the three strains is visualized in Figures S1 and S2.

Antitrypanosomal activity

The pathogenic strain *T. brucei brucei* was used to evaluate the extract of the identified fungi for their in vitro antitrypanosomal activities. In our investigation, the ethyl acetate extracts of *Cladosporium*, *Alternaria* and *Talaromyces* demonstrated a promising inhibitory effect towards *T. brucei* with IC_{50} values of 1.3, 3.2 and 3.5 µg/

mL, respectively within 72 h, which confirmed the presence of bioactive antitrypanosomal metabolites in the tested extracts.

Metabolomic analysis of the total extract of endophytic fungi associated with rosemary roots

Metabolomic analysis can be described as a highly valuable tool for identification of natural products under definite conditions. This technique mainly depends on the rapid identification of known secondary metabolites in the extracts using gas or liquid chromatography, which is combined with HR-ESI–MS or NMR spectroscopic methods[29].

In this context, metabolomic profiling of the total extract of endophytic fungi associated with rosemary roots using HR-ESI–MS was carried out. The metabolomic analysis resulted in identification of large number of metabolites belonging to variable chemical natures such as terpenes, phenolics, alkaloids, polyketides, macrolides and others (Figures S3–S8, Table S1).

The metabolomic profiling of the total extract of *Alternaria* Sp. fungus, isolated from rosemary roots, resulted in identification of seventeen compounds (Fig. 1). The mass ion peak at *m/z* 209.0785 $[M-H]^-$ was in agreement with the molecular formula $C_{11}H_{14}O_4$. It was dereplicated as phomalichenone F **(1)**, which was previously identified in the extract of *Alternaria* sp. MCCC 3A00467[30]. Another mass ion peak at *m/z* 223.0589 $[M+H]^+$ was corresponding to the molecular formula $C_{11}H_{10}O_5$. It was determined to be either *(S)*-isoochracinate A1 **(2a)** or *(R)*-isoochracinate A2 **(2b)** isomers, which were previously reported in the extract of *Alternaria* sp. SCSIO41014[31]. Similarly, the mass ion peak at *m/z* 279.0864 $[M-H]^-$ was in match with the molecular formula $C_{14}H_{16}O_6$. Thus, it was identified as either alternabenzofuran A **(3a)** or alternabenzofuran B **(3b)** isomers, which were previously isolated from the extract of *Alternaria* sp. 5102[32]. Furthermore, the mass observed at *m/z* 285.1320 $[M+H]^+$ was corresponded to the molecular formula $C_{14}H_{20}O_6$ identified as phomaligol A. Phomaligol A **(4)** was previously isolated from *Altenaria* sp.[33]. Moreover, the mass ion peak at *m/z* 307.1178 $[M-H]^-$ was in agreement with the molecular formula $C_{16}H_{20}O_6$. It was identified as one of the three stereoisomers tetrahydroaltersolanol C, D or E **(5a)**, **(5b)** or **(5c)**, respectively, which were isolated from *Alternaria sp.* ZJ-2008003[34].

Besides, the mass ion peak at *m/z* 333.1673 $[M-H]^-$ was corresponding to the molecular formula $C_{19}H_{26}O_5$. It was dereplicated either as tricycloalternarene R **(6a)**, which was previously reported in the extract of *Alternaria alternata* JJY-32[35], or methyl nortricycloalternarate **(6b)**, which was previously reported in the extract of *Alternaria alternate*[36]. Another mass ion peak at *m/z* 379.2111 $[M-H]^-$ was in agreement with the molecular formula $C_{21}H_{32}O_6$, which was identified as tricycloalterfurene C **(7)** from *Alternaria alternata* k21-1[37]. In addition, the mass ion peak at *m/z* 381.2303 $[M-H]^-$ was in match with the molecular formula $C_{21}H_{34}O_6$ and was identified either as bicycloalternarene A **(8a)** or B **(8b)** ,which were previously isolated from *Alternaria* sp. JJY-32. Another two mass ion peak at *m/z* 391.2113 and 393.2299 $[M-H]^-$ were corresponding to the molecular formulas $C_{22}H_{32}O_6$ and $C_{22}H_{34}O_6$, respectively. They were dereplicated as monocycloalternarene B **(9)** and C **(10)**, respectively, which were previously reported in the extract of *Alternaria* sp. JJY-32[38]. The last mass ion peak at *m/z* 395.2057 $[M-H]^-$ was in match with the molecular formula $C_{21}H_{32}O_7$. It was identified as tricycloalterfurene D **(11)**, which was previously isolated from *Alternaria alternata* k21-1[37].

The metabolomic analysis of the total extract of *Cladosporium* Sp. fungus, isolated from rosemary roots, resulted in identification of twenty-one compounds (Fig. 2). The mass ion peak at *m/z* 183.1393 $[M+H]^+$ was corresponding to the molecular formula $C_{11}H_{18}O_2$. It was identified as (3*E*,8*E*,6*S*)-undeca-3,8,10-trien-1,6-diol **(12)**. Another mass ion peak at *m/z* 195.0682 $[M-H]^-$ was in match with the molecular formula $C_{10}H_{12}O_4$, which was identified as (2*S*,3*S*,4*R*)-2-Methylchroman-3,4,5-triol **(13).** The two compounds **(12)** and **(13)** were previously isolated from *Cladosporium* sp. OUCMDZ-302[39]. Whereas that at *m/z* 209.0418 $[M-H]^-$ was in agreement with the molecular formula $C_{10}H_{10}O_5$. It was annotated as herbarin B **(14)**, which was previously isolated from *Cladosporium herbarum*[40]. The mass ion peak at *m/z* 211.0952 $[M+H]^+$ was corresponding to the molecular formula $C_{11}H_{14}O_4$. It was identified either as perangustol A **(15a)** or B **(15b)**, which were previously isolated from *Cladosporium perangustum* FS62[41]. Also, the mass ion peak at *m/z* 223.0939 $[M-H]^-$ was in match with the molecular formula $C_{12}H_{16}O_4$. It was dereplicated as cladosporin D **(16)**, which was previously isolated from *Cladosporium* sp. SCSIO z015[42]. Another mass ion peak at *m/z* 227.1276 $[M-H]^-$ was corresponding to the molecular formula $C_{12}H_{20}O_4$. It was identified as iso-cladospolide B **(17)**, which was previously reported in the extract of *Cladosporium* sp.[43]. Moreover, the mass ion peak at *m/z* 230.1506 $[M-H]^-$ was in agreement with the molecular formula $C_{12}H_{22}O_4$. It was dereplicated as cladospolide F **(18a)** or *ent*-cladospolide F **(18b)**, which were previously isolated from *Cladosporium* sp. TZP-29[44] and *Cladosporium cladosporioides* MA-299[45], respectively.

Besides, the mass ion peak at *m/z* 237.0747 $[M+H]^+$ was corresponding to the molecular formula $C_{12}H_{12}O_5$. It was identified as herbarin A **(19)**, which was previously reported in *Cladosporium herbarum*[40]. Another mass ion peak at *m/z* 239.0902 $[M+H]^+$ was in match with the molecular formula $C_{12}H_{14}O_5$. It was annotated as (3*R*)-3-(2-hydroxypropyl)-6,8-dihydroxy-3,4-dihydroisocoumarin **(20)**, which was previously isolated from *Cladosporium* sp. SCSIO41007[46]. The mass ion peak at *m/z* 243.1225 $[M-H]^-$ was in agreement with the molecular formula $C_{12}H_{20}O_5$. It was annotated as cladoscyclitol A **(21)**, which was previously reported from *Cladosporium* sp. JJM22[47]. Additionally, the mass ion peak at *m/z* 245.1393 $[M+H]^+$ was corresponding to the molecular formula $C_{12}H_{20}O_5$. It was identified either as pandangolide 1 **(22a)** or pandangolide 1a **(22b)**, which were previously isolated from *Cladosporium* sp.[43]**.** Similarly, the mass ion peak at *m/z* 243.1591 was annotated either as cladosporester A **(23a)** or cladosporester B **(23b)** in correspondence to the molecular formula $C_{13}H_{24}O_4$. They were previously reported in the extract of *Cladosporium cladosporioides* OUCMDZ-187[48].

In addition, the mass ion peak at *m/z* 245.1379 $[M-H]^-$ was in agreement with the molecular formula $C_{12}H_{22}O_5$. It was identified as cladoscyclitol D **(24)**, which was previously isolated from *Cladosporium* sp. JJM22[47]. Another mass ion peak at *m/z* 273.1684 $[M+H]^+$ was corresponding to the molecular formula $C_{14}H_{24}O_5$. It was dereplicated

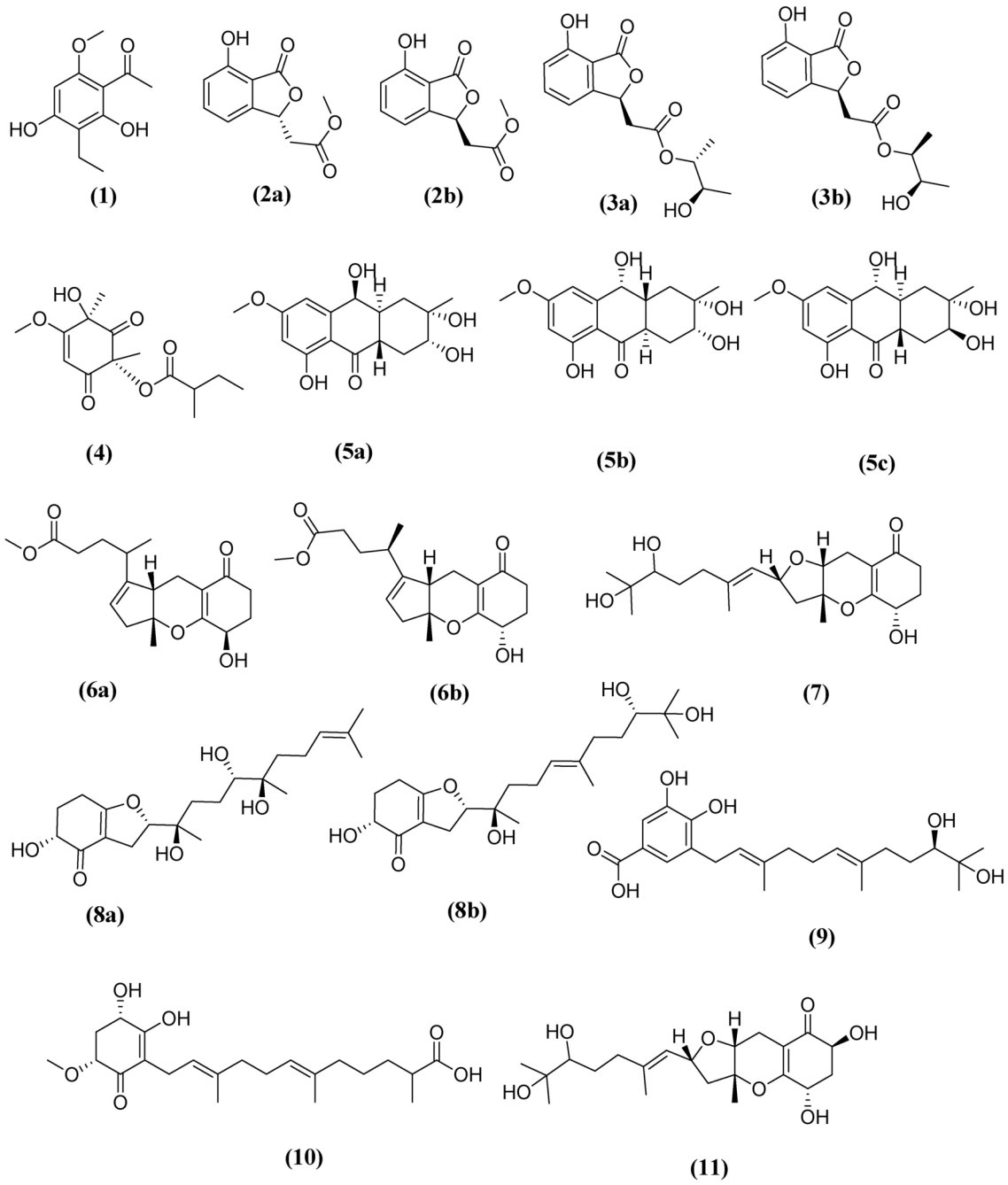

Fig. 1. The annotated metabolites from the EtOAc extract of rosemary root-derived *Alternaria* sp.

as cladospolide G **(25)**, which was previously reported in the extract of *Cladosporium cladosporioides* MA-299[45]. Moreover, the mass ion peak at *m/z* 305.1382 $[M-H]^-$ was annotated as thiocladospolide E **(26)**, which was previously isolated from *Cladosporium* sp. SCNU-F0001, with correspondence to the molecular formula $C_{14}H_{26}O_5S$[49]. Whereas that at *m/z* 417.1525 $[M-H]^-$ was in agreement with the molecular formula $C_{23}H_{22}N_4O_4$. It was identified as *epi*-cladoquinazoline **(27)**, which was previously isolated from *Cladosporium* sp. PJX-41[50]. The last mass ion peak at *m/z* 459.3097 $[M-H]^-$was identified as cladosporisteroid A **(28)**. It was in agreement with the molecular formula $C_{28}H_{44}O_5$ and previously reported in *Cladosporium* sp. SCSIO41007[46].

Concerning the metabolomic profiling of the total extract of *Talaromyces* Sp. fungus, isolated from rosemary roots, the analysis resulted in identification of twenty-four compounds (Fig. 3). The mass ion peak at *m/z* 237.0747 $[M+H]^+$ was corresponding to the molecular formula $C_{12}H_{12}O_5$. It was identified either as talamin A **(29a)** or D **(29b)**, which were previously isolated from *Talaromyces minioluteus* CS-138[51]. Similarly, the mass ion peak at *m/z* 251.1254 $[M-H]^-$ was in agreement with the molecular formula $C_{14}H_{20}O_4$. They were dereplicated as talaperoxide D **(30a)** or C **(30b)**, which were previously reported in *Talaromyces flavus*[52]. Another mass ion peak at *m/z* 267.1214 $[M-H]^-$ was in match with the molecular formula $C_{14}H_{18}O_5$. It was annotated as Methyl (*R*)-4-

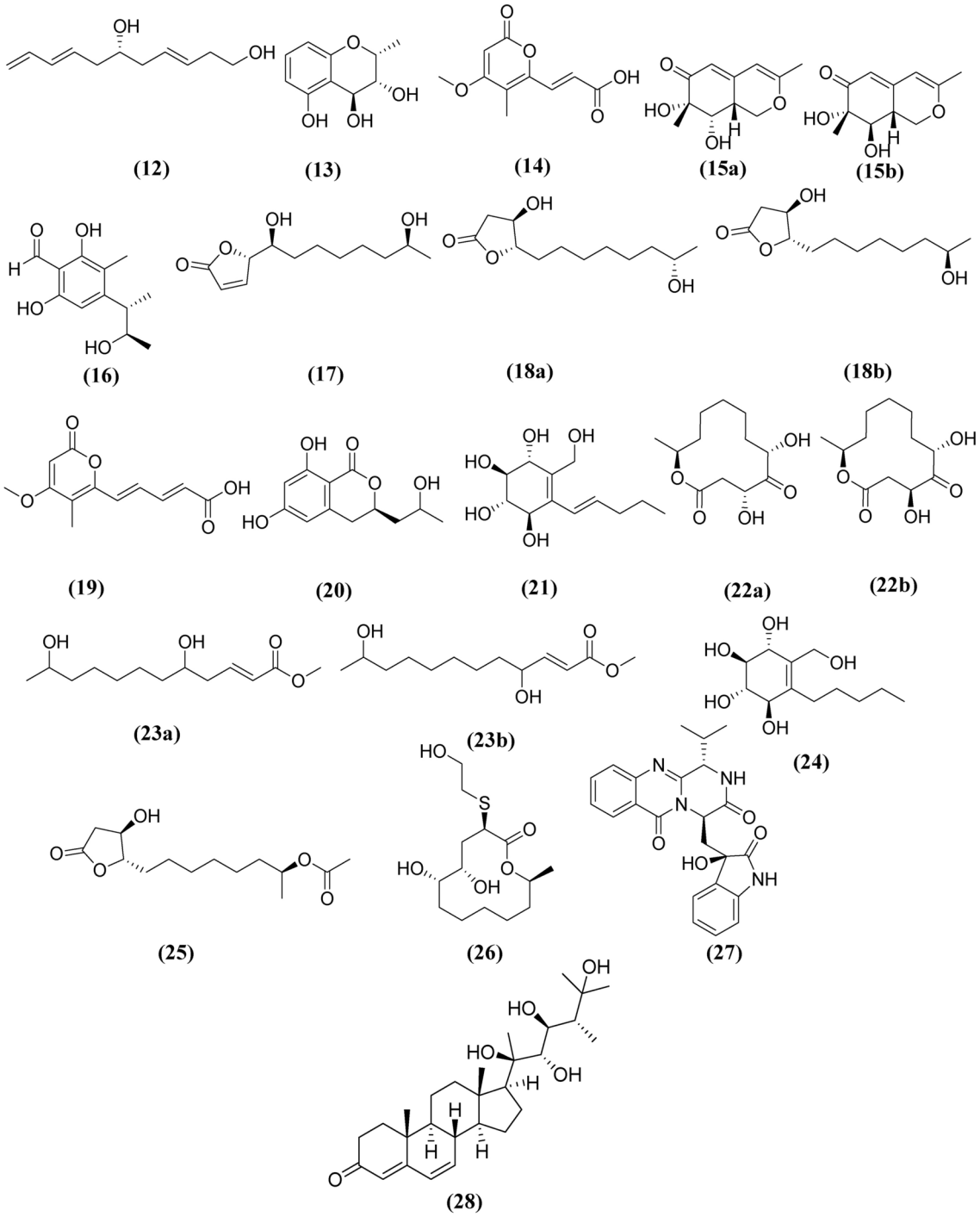

Fig. 2. The annotated metabolites from EtOAc extract of rosemary root-derived *Cladosporium* sp.

hydroxy-2-(2-hydroxypropan-2-yl)-6-methyl-2,3-dihydrobenzofuran-5-carboxylate **(31)**, which was previously isolated from *Talaromyces indigoticus* FS688[53]. Whereas that at *m/z* 289.1071 $[M-H]^-$ was identified as (3*S*)-*cis*-resorcylide **(32)** and matched with the molecular formula $C_{16}H_{18}O_5$. It was previously reported in the extract of *Talaromyces rugulosus*[55].

Moreover, the mass ion peak at *m/z* 291.1229 $[M-H]^-$ was in agreement with the molecular formula $C_{16}H_{20}O_5$. It was identified as talaromarin E **(33)**, which was previously isolated from *Talaromyces flavus*[54]. In addition, the mass ion peak at *m/z* 295.1572 $[M-H]^-$ was corresponding to the molecular formula $C_{16}H_{24}O_5$. It was dereplicated either as talaperoxide A **(34a)** or B **(34b).** They were previously reported in the extract of *Talaromyces flavus*[52]. Similarly, the mass ion peak at *m/z* 307.1178 $[M-H]^-$ was identified either as (3*S*,7*S*)-7-Hydroxyresorcylide **(35a)** or (3*S*,7*R*)-7-Hydroxyresorcylide **(35b)**. They were matched with the molecular formula $C_{16}H_{20}O_6$ and previously reported in *Talaromyces rugulosus*[55]. Also, the mass ion peak at *m/z* 321.1331

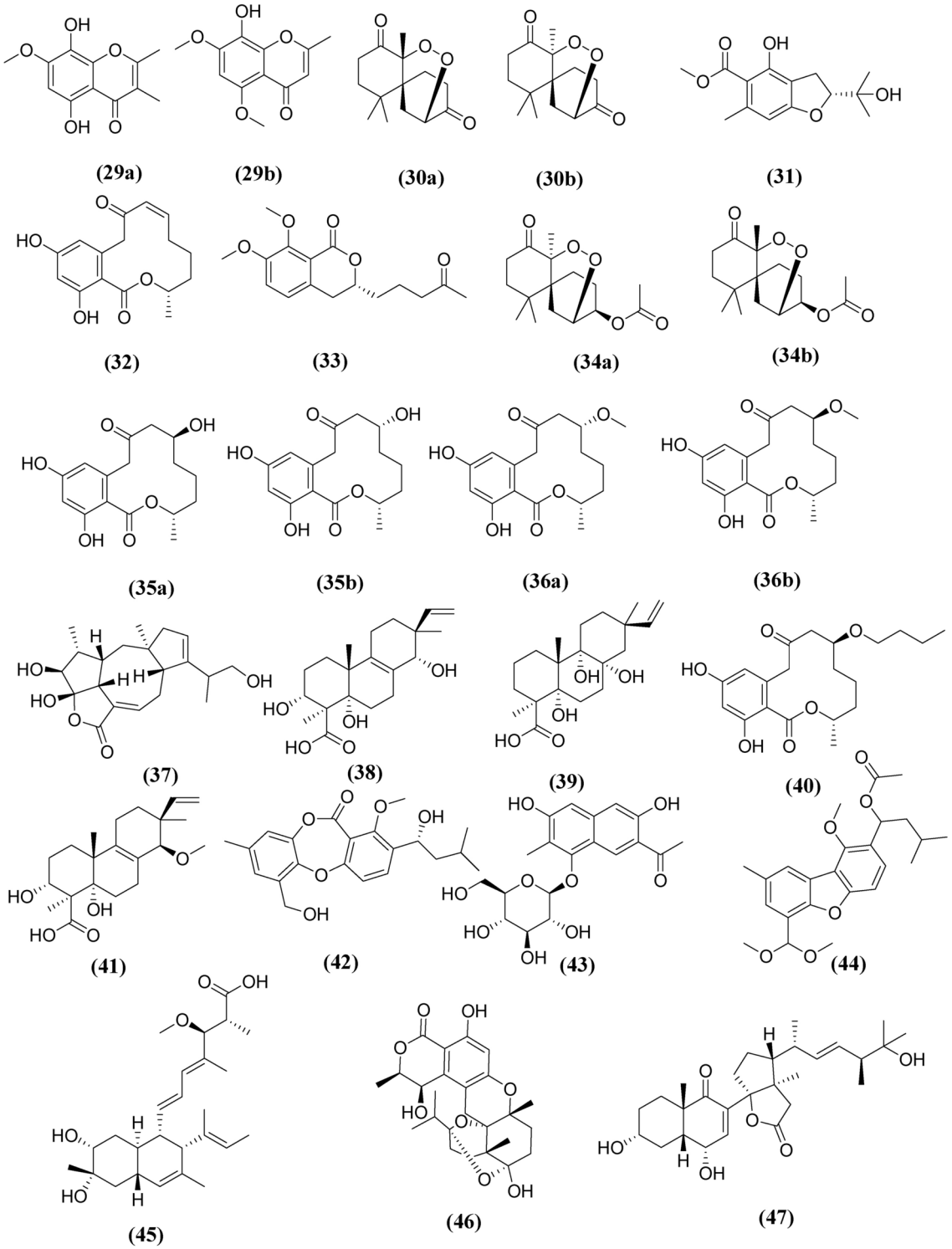

Fig. 3. The annotated metabolites from the EtOAc extract of rosemary root-derived *Talaromyces* sp.

$[M\text{-}H]^-$ was corresponding to the molecular formula $C_{17}H_{22}O_6$. It was dereplicated either as (3*S*,7*R*)-7-Methoxyresorcylide **(36a)** or (3*S*,7*S*)-7-Methoxyresorcylide **(36b).** They were previously reported in the extract of *Talaromyces rugulosus*[55].

Additionally, the mass ion peak at *m/z* 347.1847 $[M\text{-}H]^-$ was corresponding to the molecular formula $C_{20}H_{28}O_5$. It was identified as roussoellol C **(37)**, which was previously isolated from *Talaromyces purpurogenus*[56]. Another mass ion peak at *m/z* 351.2150 $[M+H]^+$ was corresponding to the molecular formula $C_{20}H_{30}O_5$. It was annotated as talascortene F **(38)**. Also, the mass ion peak at *m/z* 353.2308 $[M+H]^+$ was in match with the molecular formula $C_{20}H_{32}O_5$ and identified as talascortene C **(39)**. The two metabolites **(38)** and **(39)**, which

were previously reported in *Talaromyces scorteus* AS-242[57]. Moreover, the mass ion peak at *m/z* 363.1800 $[M-H]^-$ was in agreement with the molecular formula $C_{20}H_{28}O_6$. It was dereplicated as (3*S*,7*S*)-7-O-*n*-butylresorcylide **(40)**, which was previously isolated from *Talaromyces rugulosus*[55].

In addition, the mass ion peak at *m/z* 363.2140 $[M-H]^-$ corresponded to the molecular formula $C_{21}H_{32}O_5$. It was identified as talascortene G **(41)**, which was previously isolated from *Talaromyces scorteus* AS-242[57]. Another mass ion peak at *m/z* 371.1520 was in agreement with the molecular formula $C_{21}H_{24}O_6$. It was dereplicated as talaromyone A **(42)**, which was previously reported in the extract of *Talaromyces stipitatus* SK-4[58]. Whereas that at *m/z* 395.1328 $[M+H]^+$ was corresponding to the molecular formula $C_{19}H_{22}O_9$. It was identified as talaminioside B **(43)**, which was previously isolated from *Talaromyces minioluteus* CS-113[59]. Moreover, the mass ion peak at *m/z* 415.2099 $[M+H]^+$ was corresponding to the molecular formula $C_{24}H_{30}O_6$. It was annotated as talaromycin B **(44)**, which was previously reported in the extract of *Talaromyces* sp.[60]. Additionally, the mass ion peak at *m/z* 431.2788 $[M-H]^-$ was identified as fusarielin P **(45)**. It was previously isolated from *Talaromyces* sp. and matched with the molecular formula $C_{26}H_{40}O_5$[61]. Also, the mass ion peak at *m/z* 459.1991 $[M-H]^-$ was corresponding to the molecular formula $C_{25}H_{32}O_8$. It was identified as talaromyolide B **(46)**, which was previously reported in the extract of *Talaromyces* sp. CX11[62]. The last mass ion peak at *m/z* 473.2896 $[M-H]^-$ was in agreement with the molecular formula $C_{28}H_{42}O_6$ and dereplicated as cyclosecosteroid A **(47)**, which was previously isolated from *Talaromyces* sp. SCNU-F0041[63].

In silico molecular docking

Generally, most of the test compounds gave moderate docking score (S; kcal/mol) within rhodesain crystal structure, as shown in Table 1 on the other hand, the simulations within ornithine decarboxylase active site were some differentials between compounds of three extracts isolated from fungal strains, as number of compounds having significant docking score were in agreement with results obtained in biological investigations done, as shown in Table 1.

Commonly, after visual inspection of the best docking poses of each test compound, H-bonding and H-pi interactions were the common binding forces exerted against key amino acid residues (such as; Met 68, Gln 19, Asp 161, Asp 69, Gly 66, and Cys 25) lining active site of rhodesain (PDB ID: 6EXQ), as shown in Table S2. Examining the docking poses of either epi-cladoquinazoline, compounds **27**, and **33** as model compounds to explore potential mechanism by which such compounds could inhibit the rhodeasin catalytic activity, revealed the formation of strong H-donor bonds with both Met 68 and Cys 25 as found with co-crystallized ligand ((3 ~ {S})-19-chloranyl- ~ {N}-(1-cyanocyclopropyl)-8-methoxy-5-oxidanylidene-12,17-dioxa-4-azatricyclo[16.2.2.0^{6,11}]docosa-1(20),6(11),7,9, 18,21-hexaene-3-carboxamide) as shown in Fig. 4, which indicates high possibility of being potential inhibitors of this enzyme.

The results of antitrypanosomal investigations of the EtOAc extract of three endophytic fungi associated with rosemary roots (*Cladosporium* spp., *Alternaria* spp. and *Talaromyces* spp.) in our study proved the potential of natural products as antitrypanosomal drugs even from plant associated fungi. The potential antitrypanosomal actions of the screened extracts may be attributed to the presence of coumarins, alkaloids, and polyketides that was previously reported for their antitrypanosomal activity[64]. Correlations between the identified compounds and detected antitrypanosomal activities were proved through docking study against target protein active sites and the results demonstrated significant docking score, especially for compounds 27 and 33 (Table 1). These results were in agreement with the previously reviewed data concerning the antitrypanosomal potential of different metabolites as alkaloids[65], coumarins[64], terpenes[66] and polyketides[67].

Conclusion

The present work spotted the isolation and purification of three endophytic fungi associated with rosemary roots, in addition to the investigation of their metabolomic diversity and the antitrypanosomal activity. The isolated fungi were identified molecularly as *Cladosporium sphaerospermum* (UR1), *Alternaria papavericola* (UR2), and *Talaromyces stititatus* (UR3). Interestingly, these recovered fungal strains were able to produce a variety of metabolites through fermentation under certain conditions, as demonstrated by the LC-HR-ESI-MS metabolomic profiling. Additionally in vitro studies of the extracts of the three different fungal strains revealed their potent antitrypanosomal effects, UR1 fungal extract demonstrated the highest efficacy against *Trypanosoma brucei*, with IC_{50} value of 1.3, µg/mL. Moreover, the molecular docking supported this observation in line with the experimental activity profile and indicates that these fungal extracts could have promising compounds as inhibitors of rhodesain and ornithine decarboxylase proteins. Therefore, plant fungal endophytes have been established to gain new dimensions to provide a range of unique bio-products with a wide range of bioactivities, and this work is ongoing in search of new sources of medications.

No	Compound	6EXQ	4ZGY
1	Phomalichenone F $C_{11}H_{14}O_4$	−4.46	−3.58
2a	(S)-Isoochracinate A1 $C_{11}H_{10}O_5$	−4.55	−4.87
3a	Alternabenzofuran A $C_{14}H_{16}O_6$	−5.22	−3.7
4	Phomaligol A $C_{14}H_{20}O_6$	−4.62	NA
5a	Tetrahydroaltersolanol C $C_{16}H_{20}O_6$	−4.56	NA
6a	Tricycloalternarene R $C_{19}H_{26}O_5$	−5.03	NA
7	Tricycloalterfurene C $C_{21}H_{32}O_6$	−5.58	NA
8a	Bicycloalternarene A $C_{21}H_{34}O_6$	−5.67	−3.3
9	Monocycloalternarene B $C_{22}H_{32}O_6$	−5.77	−4.3
10	Monocycloalternarene C $C_{22}H_{34}O_6$	−5.69	−5.9
11	Tricycloalterfurene D $C_{21}H_{32}O_7$	−5.62	−4.0
12	(3E,8E,6S)-Undeca-3,8,10-trien-1,6-diol $C_{11}H_{18}O_2$	NA	NA
13	(2S,3S,4R)-2-Methylchroman-3,4,5-triol $C_{10}H_{12}O_4$	−5.55	−3.1
14	Herbarin B $C_{10}H_{10}O_5$	−4.32	−5.01
15a	Perangustol A $C_{11}H_{14}O_4$	−4.36	−4.3
16	Cladosporin D $C_{12}H_{16}O_4$	NA	−3.97
17	Iso-Cladospolide B $C_{12}H_{20}O_4$	−4.91	−4.98
18a	Cladospolide F $C_{12}H_{22}O_4$	−5.20	−4.87
19	Herbarin A $C_{12}H_{12}O_5$	−5.21	−4.02
20	(3R)-3-(2-Hydroxypropyl)-6,8-dihydroxy-3,4-dihydroisocoumarin $C_{12}H_{14}O_5$	−4.29	−3.66
21	Cladoscyclitol A $C_{12}H_{20}O_5$	−4.75	−3.31
22a	Pandangolide 1 $C_{12}H_{20}O_5$	−5.04	NA
23a	Cladosporester A $C_{13}H_{24}O_4$	NA	NA
24	Cladoscyclitol D $C_{12}H_{22}O_5$	−4.51	−3.08
25	Cladospolide G $C_{14}H_{24}O_5$	−4.65	−3.77
26	Thiocladospolide E $C_{14}H_{26}O_5S$	−5.71	NA
27	epi-Cladoquinazoline $C_{23}H_{22}N_4O_4$	−6.00	NA
28	Cladosporisteroid A $C_{28}H_{44}O_5$	−5.99	NA
29a	Talamin A $C_{12}H_{12}O_5$	−5.17	−2.33
29b	Talamin D $C_{12}H_{12}O_5$	NA	NA
30a	Talaperoxide D $C_{14}H_{20}O_4$	−4.91	NA
31	Methyl (R)-4-hydroxy-2-(2-hydroxypropan-2-yl)-6-methyl-2,3-dihydrobenzofuran-5-carboxylate $C_{14}H_{18}O_5$	−4.46	NA
32	(3S)-cis-Resorcylide $C_{16}H_{18}O_5$	−4.14	−5.4
Continued			

No	Compound	6EXQ	4ZGY
33	Talaromarin E $C_{16}H_{20}O_5$	−5.19	NA
34a	Talaperoxide A $C_{16}H_{24}O_5$	−3.95	NA
35a	(3S,7S)-7-Hydroxyresorcylide $C_{16}H_{20}O_6$	−4.43	NA
36a	(3S,7R)-7-Methoxyresorcylide $C_{17}H_{22}O_6$	−4.65	NA
37	Roussoellol C $C_{20}H_{28}O_5$	−4.88	NA
38	Talascortene F $C_{20}H_{30}O_5$	−3.91	NA
39	Talascortene C $C_{20}H_{32}O_5$	−3.82	NA
40	(3S,7S)-7-O-n-Butylresorcylide C20H28O6	−4.78	NA
41	Talascortene G $C_{21}H_{32}O_5$	−4.67	NA
42	Talaromyone A $C_{21}H_{24}O_6$	−6.10	NA
43	Talaminioside B $C_{19}H_{22}O_9$	*−5.57*	NA
44	Talaromycin B $C_{24}H_{30}O_6$	−5.39	NA
45	Fusarielin P $C_{26}H_{40}O_5$	*−4.98*	−5.44
46	Talaromyolide B $C_{25}H_{32}O_8$	−4.58	NA
47	Cyclosecosteroid A $C_{28}H_{42}O_6$	−3.95	NA

Table 1. Docking score of the tested compounds (s; kcal/mol) within both Rhodesain and ornithine decarboxylase active sites.

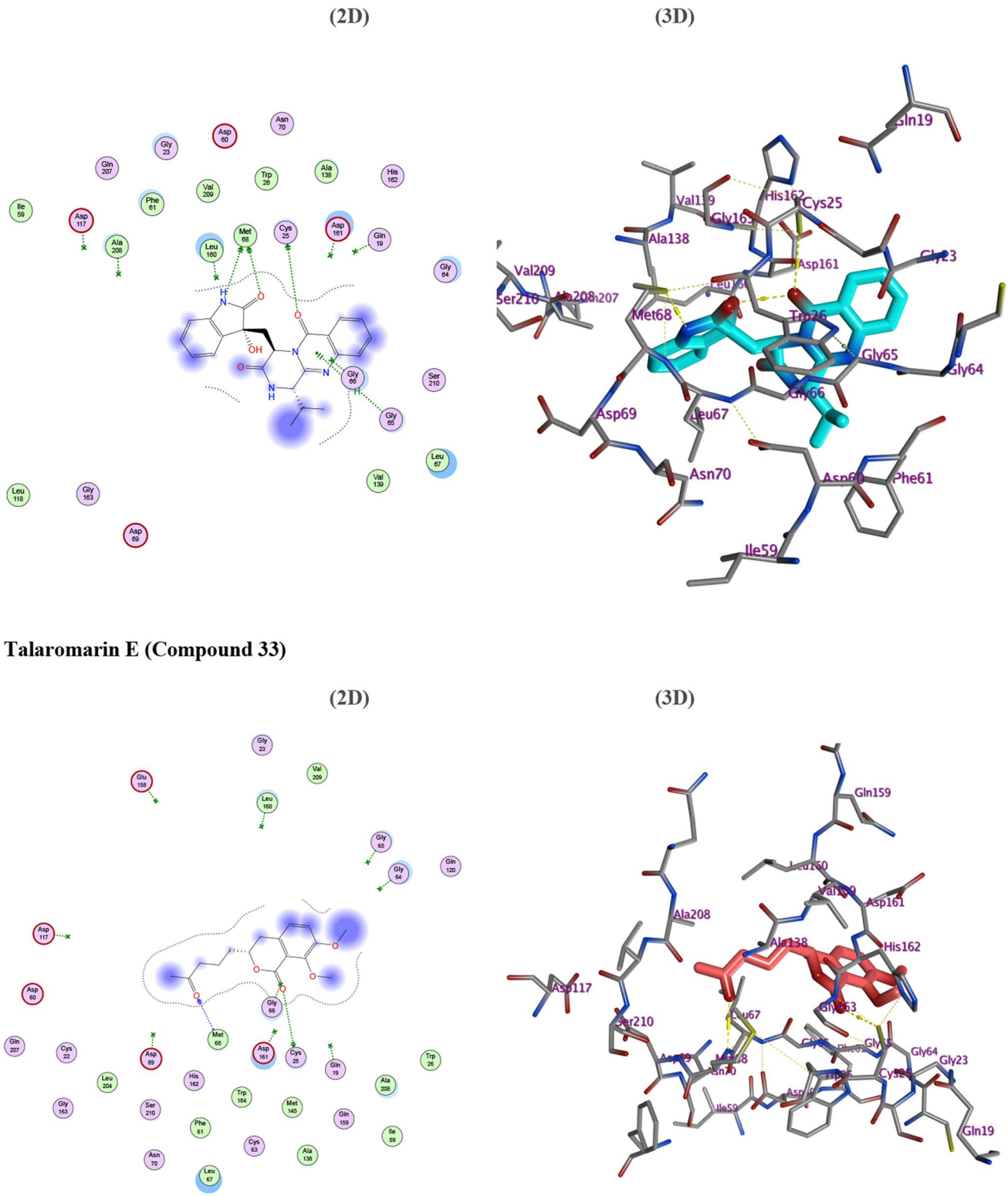

Fig. 4. 2D & 3D Sketch of Binding Interactions of 27 (cyan-blue) and 33 (pink) showing H-bonds (yellow arrows) with Met 68 and Cys 25 of Rhodesain Active Site (PDB ID: 6EXQ).

Data availability

All data generated or analyzed during this study are included in this published article (and its supplementary information files).

Received: 25 October 2024; Accepted: 12 February 2025
Published online: 15 May 2025

References

1. Suryanarayanan, T. S. et al. Fungal endophytes and bioprospecting. *Fungal Biol. Rev.* **23**, 9–19 (2009).
2. Aly, A. H., Debbab, A. & Proksch, P. Fungal endophytes: Unique plant inhabitants with great promises. *Appl. Microbiol. Biotechnol.* **90**, 1829–1845 (2011).
3. Gutierrez, R. M., Gonzalez, A. M. & Ramirez, A. M. Compounds derived from endophytes: A review of phytochemistry and pharmacology. *Curr. Med. Chem.* **19**, 2992–3030 (2012).
4. Fernández-pastor, I. & González-menendez, V. Pipecolisporin, a novel cyclic peptide with antimalarial and antitrypanosome activities from a wheat endophytic *Nigrospora oryzae*. *Pharmaceuticals* **14**, 1–9 (2021).
5. Pina, J. R. S. et al. Antiprotozoal and antibacterial activity of ravenelin, a xanthone isolated from the endophytic fungus *Exserohilum rostratum*. *Molecules* **26**, 1–11 (2021).
6. Pays, E., Radwanska, M. & Magez, S. The pathogenesis of African trypanosomiasis. *Ann. Rev. Pathol. Mech. Dis.* **18**(1), 19–45 (2023).
7. Steverding, D. The history of African trypanosomiasis. *Parasit. Vectors* **1**, 3 (2008).
8. Ungogo, M. A. et al. A review of the antimalarial, antitrypanosomal, and antileishmanial activities of natural compounds isolated from Nigerian flora. *Front. Chem.* **8**, 1–28 (2020).
9. Aly, A. H. et al. NF kappa B inhibitors and antitrypanosomal metabolites from endophytic fungus *Penicillium* sp. isolated from *Limonium tubiflorum*. *Bioorg. Med. Chem.* **19**, 414–421 (2011).
10. Cota, B. B. et al. Altenusin, a biphenyl isolated from the endophytic fungus *Alternaria* sp., inhibits trypanothione reductase from *Trypanosoma cruzi*. *FEMS Microbiol. lett.* **285**, 177–182 (2008).
11. Diyaolu, O. A. et al. Antiparasitic activities of compounds isolated from *Aspergillus fumigatus* strain discovered in Northcentral Nigeria. *Antibiotics* **12**, 1–16 (2023).
12. Farouk, H. M., Attia, E. Z. & El-katatny, M. M. H. Hydrolytic enzyme production of endophytic fungi isolated from soybean (Glycine max). *J. Mod. Res.* **2**, 1–7 (2020).
13. Shady, N. H. et al. Phytochemical analysis and anti-infective potential of fungal endophytes isolated from *Nigella sativa* seeds. *BMC Microbiol.* **23**, 343 (2023).
14. Sayed, A. M. et al. Metabolomic profiling and antioxidant potential of three fungal endophytes derived from *Artemisia annua* and *Medicago sativa*. *Nat. Prod. Res.* **36**, 2404–2408 (2020).
15. Mohie El-dien, T. R. et al. *Paralemnalia thyrsoides*-associated fungi: Phylogenetic diversity, cytotoxic potential, metabolomic profiling and docking analysis. *BMC Microbiol.* **23**, 1–12 (2023).
16. May, L. A., Smiley, B. & Schmidt, M. G. Comparative denaturing gradient gel electrophoresis analysis of fungal communities associated with whole plant corn silage. *Can. J. Microbiol.* **47**, 829–841 (2001).
17. White, T. J., Bruns, T. D., Lee, S. J. W. & Taylor, J. Amplification and direct sequencing of fungal ribosomal RNA genes for phylogenetics. In *PCR Protocols: A Guide to Methods and Applications* (eds Innis, M. A. & Gelfand, D. H.) (Academic Press, 1990).
18. Tamura, K., Stecher, G. & Kumar, S. MEGA 11: Molecular evolutionary genetics analysis version 11. *Mol. Biol. Evol.* **38**, 3022–3027 (2021).
19. Stecher, G., Tamura, K. & Kumar, A. S. Molecular evolutionary genetics analysis (MEGA) for macOS. *Mol. Biol. Evol.* **37**, 1237–1239 (2020).
20. Thompson, J. D., Higgins, D. G. & Gibson, A. T. J. J. N. A. R. CLUSTAL W: Improving the sensitivity of progressive multiple sequence alignment through sequence weighting, position-specific gap penalties and weight matrix choice. *Nucleic Acids Res.* **22**, 4673–4680 (1994).
21. Nei, M. & Kumar, S. *Molecular Evolution and Phylogenetics* (Oxford University Press, 2000).
22. Kimura, M. A simple method for estimating evolutionary rates of base substitutions through comparative studies of nucleotide sequences. *J. Mol. Evol.* **16**, 111–120 (1980).
23. Abdelmohsen, U. R. et al. Dereplication strategies for targeted isolation of new antitrypanosomal actinosporins A and B from a marine sponge associated-*Actinokineospora* sp. EG49. *Mar. Drugs* **12**, 1220–1244 (2014).
24. Pluskal, T., Castillo, S., Villar-briones, A. & Oresic, M. MZmine 2: Modular framework for processing, visualizing, and analyzing mass spectrometry-based molecular profile data. *BMC Bioinformatics* **11**, 395 (2010).
25. Abboud, M., Rybchyn, M., Rizk, R., Fraser, D. & Mason, R. Sunlight exposure is just one of the factors which influence vitamin D status. *Photochem. Photobiol. Sci.* **16**, 302–313 (2017).
26. Molecular Operating Environment (MOE). 2010.10, Chemical Computing Group Inc. (2012).
27. Abdelmohsen, U. R. et al. Naturally occurring phenylethanoids and phenylpropanoids: Antimalarial potential. *RSC Adv.* **13**, 26804–26811 (2023).
28. Huber, W. & Koella, J. C. A comparison of three methods of estimating EC_{50} in studies of drug resistance of malaria parasites. *Acta. Trop.* **55**, 257–261 (1993).
29. Macintyre, L. et al. Metabolomic tools for secondary metabolite discovery from marine microbial symbionts. *Mar. Drugs* **12**, 3416–3448 (2014).
30. Zhong, T. H. et al. Three new phomalone derivatives from a deep-sea-derived fungus *Alternaria* sp. MCCC 3A00467. *Nat. Prod. Res.* **36**, 414–418 (2022).
31. Pang, X. et al. Perylenequione derivatives with anticancer activities isolated from the marine sponge-derived fungus, *Alternaria* sp. SCSIO41014. *Mar. Drugs* **16**, 1–7 (2018).
32. Chen, S. et al. Secondary metabolites with nitric oxide inhibition from marine-derived fungus *Alternaria* sp. 5102. *Mar. Drugs* **18**, 1–14 (2020).
33. Li, X. et al. γ-Pyrone derivatives, kojic acid methyl ethers from a marine-derived *fungusaltenaria* sp. *Arch. Pharm. Res.* **26**, 532–534 (2003).
34. Zheng, C. J. et al. Bioactive hydroanthraquinones and anthraquinone dimers from a soft coral-derived *Alternaria* sp. Fungus. *J. Nat. Prod.* **75**, 189–197 (2012).
35. Liu, G. et al. Overexpression of transcriptional regulator and tailoring enzyme leads to the discovery of anti-inflammatory meroterpenoids from marine-derived fungus *Alternaria alternata* JJY-32. *Front. Mar. Sci.* **9**, 1–11 (2022).
36. Shi, Z. Z., Fang, S. T., Miao, F. P. & Ji, N. Y. Two new tricycloalternarene esters from an alga-epiphytic isolate of *Alternaria alternata*. *Nat. Prod. Res.* **32**, 2523–2528 (2018).
37. Shi, Z. et al. Sesteralterin and Tricycloalterfurenes A-D: Terpenes with rarely occurring frameworks from the marine-alga-epiphytic fungus *Alternaria alternata* k21–1. *J. Nat. Prod.* **80**, 2524–2529 (2017).

38. Zhang, G. et al. Meroterpenoids with diverse ring systems from the sponge-associated fungus *Alternaria* sp. JJY-32. *J. Nat. Prod.* **76**, 1946–1957 (2013).
39. Wang, L. et al. Polyketides from the endophytic fungus *Cladosporium* sp. isolated from the mangrove plant *Excoecaria agallocha*. *Front. Chem.* **6**, 1–9 (2018).
40. Jadulco, R. et al. New metabolites from sponge-derived fungi *Curvularia lunata* and *Cladosporium herbarum*. *J. Nat. Prod.* **65**, 730–733 (2002).
41. Fan, Z. et al. Perangustols A and B, a pair of new azaphilone epimers from a marine sediment-derived fungus *Cladosporium perangustm* FS62. *J. Asian. Nat. Prod. Res.* **18**, 1024–1029 (2016).
42. Amin, M., Zhang, X. Y., Xu, X. Y. & Qi, S. H. New citrinin derivatives from the deep-sea-derived fungus *Cladosporium* sp. SCSIO z015. *Nat. Prod. Res.* **34**, 1219–1226 (2020).
43. Gesner, S., Cohen, N., Ilan, M., Yarden, O. & Carmeli, S. Pandangolide 1a, a metabolite of the sponge-associated fungus *Cladosporium* sp., and the absolute stereochemistry of Pandangolide 1 and iso-Cladospolide B. *J. Nat. Prod.* **68**, 1350–1353 (2005).
44. Zhu, M. et al. Lipid-lowering polyketides from a soft coral-derived fungus *Cladosporium* sp. TZP29. *Bioorg. Med. Chem. Lett.* **25**, 3606–3609 (2015).
45. Zhang, F. Z. et al. Polyketides from the mangrove-derived endophytic fungus *Cladosporium cladosporioides*. *Mar. Drugs* **17**, 1–13 (2019).
46. Pang, X. et al. Three new highly oxygenated sterols and one new dihydroisocoumarin from the marine sponge-derived fungus *Cladosporium* sp. SCSIO41007. *Steroids* **129**, 41–46 (2018).
47. Zhang, B. et al. Bioactive cyclohexene derivatives from a mangrove-derived fungus *Cladosporium* sp. JJM22. *Fitoterapia* **149**, 104823 (2021).
48. Peng, X., Wang, Y., Zhu, G. & Zhu, W. Fatty acid derivatives from the halotolerant fungus *Cladosporium cladosporioides*. *Magn. Reson. Chem.* **56**, 18–24 (2018).
49. Huang, C. et al. Thiocladospolide E and cladospamide A, novel 12-membered macrolide and macrolide lactam from mangrove endophytic fungus *Cladosporium* sp. SCNU-F0001. *Fitoterapia* **137**, 104246 (2019).
50. Peng, J. et al. Antiviral alkaloids produced by the mangrove-derived fungus *Cladosporium* sp. PJX-41. *J. Nat. Prod.* **76**, 1133–1140 (2013).
51. Song, Q. et al. Aromatic polyketides from the deep-sea cold-seep mussel associated endozoic fungus *Talaromyces minioluteus* CS-138. *Mar. Drugs* **20**, 1–9 (2022).
52. Li, H. et al. Cytotoxic norsesquiterpene peroxides from the endophytic fungus *Talaromyces flavus* isolated from the mangrove plant *Sonneratia apetala*. *J. Nat. Prod.* **74**, 1230–1235 (2011).
53. Liu, Z. et al. Molecular networking-based discovery of new polyketides from the deep-sea-derived fungus *Talaromyces indigoticus* FS688. *Tetrahedron* **138**, 133410 (2023).
54. Cai, J. et al. Talaromarins A–F: Six new isocoumarins from mangrove-derived fungus *Talaromyces flavus* TGGP35. *Mar. Drugs* **20**, 1–13 (2022).
55. Kuppers, L. et al. Lactones from the sponge-derived fungus *Talaromyces rugulosus*. *Mar. Drugs* **15**, 1–16 (2017).
56. Wang, W. et al. Two new terpenoids from *Talaromyces purpurogenus*. *Mar. Drugs* **16**, 1–10 (2018).
57. Meng, L. H., Li, X. M., Zhang, F. Z., Wang, Y. N. & Wang, B. G. Talascortenes A-G, highly oxygenated diterpenoid acids from the sea-anemone-derived endozoic fungus *Talaromyces scorteus* AS-242. *J. Nat. Prod.* **83**, 2528–2536 (2020).
58. Cai, R. et al. Depsidones from *Talaromyces stipitatus* SK-4, an endophytic fungus of the mangrove plant *Acanthus ilicifolius*. *Phytochem. Lett.* **20**, 196–199 (2017).
59. Yang, S. Q. et al. Antimicrobial polyketides and sesquiterpene lactones from the deep-sea cold-seep-derived fungus *Talaromyces minioluteus* CS-113 triggered by the histone deacetylase inhibitor SAHA. *Org. Biomol. Chem.* **21**, 2575–2585 (2023).
60. Chen, M., Han, L., Shao, C. L., She, Z. G. & Wang, C. Y. Bioactive diphenyl ether derivatives from a Gorgonian-derived fungus *talaromyces* sp. *Chem. Biodivers.* **12**, 443–450 (2015).
61. Liu, G., Huo, R., Niu, S., Song, F. & Liu, L. Two new cytotoxic decalin derivatives from marine-derived fungus *Talaromyces* sp. *Chem. Biodivers.* **19**, e202100990 (2022).
62. Cao, X. et al. Talaromyolides A-D and Talaromytin: Polycyclic meroterpenoids from the fungus *Talaromyces* sp. CX11. *Org. Lett.* **21**, 6539–6542 (2019).
63. Li, J. et al. New steroid and isocoumarin from the mangrove endophytic fungus *Talaromyces* sp. SCNU-F0041. *Molecules* **27**, 1–9 (2022).
64. Pizzolatti, M. G. et al. Trypanocidal activity of coumarins and styryl-2-pyrones from Polygala sabulosa AW Bennett (Polygalaceae). *Rev. Bras. Farmacogn.* **18**, 177–182 (2008).
65. Cavin, J. C., Krassner, S. M. & Rodriguez, E. Plant-derived alkaloids active against *Trypanosoma cruzi*. *J. Ethnopharmacol.* **19**, 89–94 (1987).
66. Otoguro, K. et al. In vitro antitrypanosomal activity of plant terpenes against *Trypanosoma brucei*. *Phytochemistry* **72**, 2024–2030 (2011).
67. Taguchi, R. & Iwasaki, A. Isolation and total synthesis of Beru'amide, an antitrypanosomal polyketide from a marine *Cyanobacterium Okeania* sp. *Org. Lett.* **24**, 4710–4714 (2022).

Acknowledgements

The authors thank the Deanship of Scientific Research at King Khalid University for funding this work through large Groups (Project under grant number R.G.P. 2/ 217 /44). And we thank Deraya University for laboratory space.

Author contributions

Conceptualization, A.M.A and U.R.A; methodology U.R.A, A.A.G, E.R.A, O.M.H, N.H.S, R.I.B, R.Y and Y.A.M; Software, U.R.A, S.P.G and P.K; supervision, A.M.A and U.R.A; data curation, U.R.A, A.A.G and E.R.A; writing, original draft preparation, All authors; writing—review and editing.

Declarations

Competing interests

The authors declare no competing interests.

Additional information

Supplementary Information The online version contains supplementary material available at https://doi.org/10.1038/s41598-025-90304-9.

Correspondence and requests for materials should be addressed to U.R.A.

Reprints and permissions information is available at www.nature.com/reprints.

Publisher's note Springer Nature remains neutral with regard to jurisdictional claims in published maps and institutional affiliations.

Open Access This article is licensed under a Creative Commons Attribution-NonCommercial-NoDerivatives 4.0 International License, which permits any non-commercial use, sharing, distribution and reproduction in any medium or format, as long as you give appropriate credit to the original author(s) and the source, provide a link to the Creative Commons licence, and indicate if you modified the licensed material. You do not have permission under this licence to share adapted material derived from this article or parts of it. The images or other third party material in this article are included in the article's Creative Commons licence, unless indicated otherwise in a credit line to the material. If material is not included in the article's Creative Commons licence and your intended use is not permitted by statutory regulation or exceeds the permitted use, you will need to obtain permission directly from the copyright holder. To view a copy of this licence, visit http://creativecommons.org/licenses/by-nc-nd/4.0/.

© The Author(s) 2025